AMP-activated protein kinase (AMPK) activity is not required for neuronal development but regulates axogenesis during metabolic stress

Tyisha Williams[a,1], Julien Courchet[b,1], Benoit Viollet[c,d,e], Jay E. Brenman[a,f,2], and Franck Polleux[b,2]

[a]Neuroscience Center, [f]Department of Cell and Developmental Biology, University of North Carolina, Chapel Hill, NC 27599; [b]Dorris Neuroscience Center, Department of Cell Biology, The Scripps Research Institute, La Jolla, CA 92037; [c]Institut National de la Santé et de la Recherche Médicale, U1016, Institut Cochin, 75014 Paris, France; [d]Centre National de la Recherche Scientifique, UMR8104, 75014 Paris, France; and [e]Université Paris Descartes, 75014 Paris, France

Edited* by Yuh-Nung Jan, Howard Hughes Medical Institute, San Francisco, CA, and approved February 28, 2011 (received for review September 13, 2010)

Mammalian brain connectivity requires the coordinated production and migration of billions of neurons and the formation of axons and dendrites. The LKB1/Par4 kinase is required for axon formation during cortical development in vivo partially through its ability to activate SAD-A/B kinases. LKB1 is a master kinase phosphorylating and activating at least 11 other serine/threonine kinases including the metabolic sensor AMP-activated protein kinase (AMPK), which defines this branch of the kinome. A recent study using a gene-trap allele of the β1 regulatory subunit of AMPK suggested that AMPK catalytic activity is required for proper brain development including neurogenesis and neuronal survival. We used a genetic loss-of-function approach producing AMPKα1/α2-null cortical neurons to demonstrate that AMPK catalytic activity is not required for cortical neurogenesis, neuronal migration, polarization, or survival. However, we found that application of metformin or AICAR, potent AMPK activators, inhibit axogenesis and axon growth in an AMPK-dependent manner. We show that inhibition of axon growth mediated by AMPK overactivation requires TSC1/2-mediated inhibition of the mammalian target of rapamycin (mTOR) signaling pathway. Our results demonstrate that AMPK catalytic activity is not required for early neural development in vivo but its overactivation during metabolic stress impairs neuronal polarization in a mTOR-dependent manner.

AMP-activated kinase (AMPK) is a heterotrimeric serine/threonine protein kinase composed of one catalytic subunit (encoded by α1 or α2 genes in mammals) and two regulatory subunits β and γ (encoded by β1 or β2 genes and γ1, γ2, or γ3 genes, respectively) (1–3). AMPK is an important metabolic sensor, activated by various forms of metabolic stress including low ATP:AMP ratios. AMPK has been implicated in a range of cell biological functions including cell polarity, autophagy, apoptosis, and cell migration (2–9). A recent study (10) suggested that the regulatory subunit, AMPKβ1, is critical for normal neurogenesis, neuronal differentiation, and neuronal survival during cortical development. However, to date there is no published evidence reporting the consequence of a genetic loss of function for the catalytic activity of mammalian AMPK in the mammalian nervous system. To assess the role of AMPKα during cortical development, we used transgenic mice that were ubiquitously inactivated for the AMPKα1 gene (AMPKα1$^{-/-}$) (11) and conditionally inactivated for AMPKα2 (AMPKα2$^{F/F}$) (12, 13). AMPKα2 was selectively deleted using the Emx1^{Cre} mouse line, which induces recombination only in dorsal telencephalic progenitors giving rise to all pyramidal projection neurons in the cortex, but not in ventral telencephalon-derived cortical GABAergic interneurons, which constitutes ∼25% of all cortical neurons (14). Surprisingly, we found no obvious defect of neurogenesis, neuronal migration, axon formation, or neuronal survival in AMPKα1/2-null cortex compared with control mice. On the basis of the profound differences between the phenotypes observed in LKB1-null neurons (15, 16) and the AMPK-null neurons (present study), we conclude that (*i*) under normal conditions, AMPK is not required for neurogenesis, neuronal differentiation, or neuronal survival in vivo; (*ii*) LKB1 function does not require AMPK catalytic activity to control neuronal polarization and survival but that (*iii*) metabolic stress inhibits axon formation during neuronal polarization as well as axon growth in an AMPK- and mammalian target of rapamycin (mTOR)-dependent manner.

Results

Genetic Loss-of-Function Approach Deleting AMPKα1/α2 Catalytic Subunits in Cortical Neurons. We first documented the pattern of expression of AMPKα1 [Mouse Genome Informatics (MGI): Prkaa1] and AMPKα2 (MGI: Prkaa2) during cortical development using RT-PCR (Fig. S1*A*) and found that both genes are expressed throughout embryonic and postnatal development and in the adult cortex. Interestingly, whereas mRNA expression levels of AMPKα1 seem rather constant at all stages examined, levels of AMPKα2 seem more tightly regulated developmentally with low levels at embryonic day (E)15.5 and peak levels during the first week of postnatal development. We confirmed these results at the protein level using an antibody that recognizes both total AMPKα1 and α2 (Fig. S1*B*). Interestingly, the level of AMPK activation measured by detection of phosphoT172-AMPK is high from E15.5 to postnatal day 1 (P1) but decreases significantly during postnatal development until adulthood (Fig. S1*B*). Several well-characterized substrates of AMPK such as ACC and $GABA_B$ receptor 2 display drastically different temporal patterns of phosphorylation. ACC phosphorylation is high from E15 to P7 but low after P15 and in adult cortex, whereas $GABA_B$ R2 phosphorylation on S783, which is entirely mediated by AMPK (Fig. S1*F*), is almost undetectable from E15 to P1. However, $GABA_B$ R2 phosphorylation increases progressively from P7 to adulthood, nicely correlating with synaptogenesis in the cortex. Finally, to circumvent the mixed nature of cell types encountered in the cortex at different stages (neurons, astrocytes, oligodendrocytes, etc.) we placed E18 cortical progenitors in culture conditions that strongly enrich for postmitotic pyramidal neurons with very limited astrocytes and oligodendrocytes. This analysis confirms that AMPK is expressed and activated rather constantly during early neuronal differentiation in vitro but its level of activation decreases sharply after 5 d in vitro (div) (Fig. S1*C*), mimicking observations at early postnatal stages in vivo (after P1; Fig. S1*B*). Taken together, the expression data show that AMPK is expressed in cortical neurons throughout development and in adulthood, but that its activation and ability to phosphorylate downstream targets is tightly regulated temporally.

Author contributions: T.W., J.C., J.E.B., and F.P. designed research; T.W. and J.C. performed research; T.W., J.C., and B.V. contributed new reagents/analytic tools; T.W., J.C., J.E.B., and F.P. analyzed data; and T.W., J.C., J.E.B., and F.P. wrote the paper.

The authors declare no conflict of interest.

*This Direct Submission article had a prearranged editor.

Freely available online through the PNAS open access option.

[1]T.W. and J.C. contributed equally to this work.

[2]To whom correspondence may be addressed. E-mail: polleux@scripps.edu or brenman@med.unc.edu.

This article contains supporting information online at www.pnas.org/lookup/suppl/doi:10.1073/pnas.1013660108/-/DCSupplemental.

NEUROSCIENCE

We generated a cortex-specific genetic ablation of AMPK catalytic activity by crossing a constitutive AMPKα1 knockout mouse with a mouse carrying an AMPKα2^{F} conditional allele. Recombination of the AMPKα2^{F} allele specifically in cortical progenitors giving rise to all pyramidal neurons was achieved by crossing with an Emx1^{Cre} mouse (14). We next validated that our genetic approach by harvesting cortical lysates from P3 Emx1$^{Cre/+}$; AMPKα1$^{-/-}$α2$^{F/F}$ mice (hereafter referred to as AMPKα-double conditional knockout, DcKO). Western blot analysis shows that total AMPKα (1 + 2) protein expression level is reduced by 70% compared with control littermates (Emx1$^{Cre/+}$; AMPKα1$^{+/-}$α2$^{F/F}$ or Emx1^{Cre}; AMPKα1$^{+/+}$α2$^{F/F}$, n = 3) (Fig. S1*D*). To evaluate protein levels without contribution from astrocytes, cortical interneurons, and blood vessels, we dissociated cultures of E15 dorsal telencephalic progenitors for 4 div. In these conditions, more than 90% of cells in culture are postmitotic glutamatergic pyramidal neurons and the cultures are almost completely devoid of radial glial progenitors or astrocytes when cultured in serum-free conditions (17, 18). Under these culture conditions, we have enriched for postmitotic pyramidal cortical neurons where Emx1^{Cre} should efficiently induce Cre-recombination and our Western blot analysis reveals a complete loss of AMPKα protein expression in the AMPKα-DcKO compared with control mice (Fig. S1*E*). To confirm the in vivo ablation of the catalytic activity of AMPK, we used phospho-specific antibodies detecting two previously characterized AMPK protein substrates: serine 783 of the GABA$_B$ receptor 2 (19) and retinoblastoma (Rb) protein on serines 807 and 811 (10). Phosphorylation of both of these proteins is abolished in the P3 cortex of AMPKα-DcKO compared with control mice (Fig. S1 *F* and *G*). These results demonstrate that our genetic approach generates a complete loss of AMPK catalytic activity in cortical pyramidal neurons in vivo.

AMPK Catalytic Activity Is Not Required for Proper Cortical Development in Vivo. AMPKα-DcKO mice are viable at birth and several individuals survived until adulthood. This allowed us to examine several aspects of cortical development at early postnatal stages. At P3, analysis of the expression of layer-specific markers such as CTIP2 (layer 5 marker), Cux1 (layer 2–4 marker) and Tbr1 (layer 6a marker) revealed no difference in layer formation between the AMPKα-DcKO (Fig. 1 *A′*–*H′*) compared with control littermates (Fig. 1 *A*–*H*). This strongly argues that AMPKα is not required for proper neurogenesis and neuronal migration in vivo. Loss of function of LKB1 (a major activator of AMPK through its ability to phosphorylate T172) and loss of function of AMPKβ1 were both reported to lead to significant levels of neuronal apoptosis in vivo (10, 15). In contrast, we found that neuronal apoptosis, as measured by the number of activated caspase 3-positive cells, is low in AMPKα-DcKO (Fig. 1 *I′*–*L′*) and not different from control littermates (Fig. 1 *I*–*L*). Finally, axon-specific (Tau1) and dendrite-specific (MAP2) marker analysis revealed no difference between the AMPKα-DcKO (Fig. 1 *M′*–*P′*) and control littermates (Fig. 1 *M*–*P*), suggesting no gross abnormalities in neuronal polarization and axon–dendrite growth. This contrasts with the phenotype observed in LKB1 cKO as well as in two other effectors of LKB1, namely SAD-A/B kinase DKO mice, where cortical pyramidal neurons do not form axons (15, 20).

To directly visualize neuronal morphology and axon–dendrite polarization, we used two alternative approaches. First we performed ex utero cortical electroporation (EUCE) on AMPKα1$^{-/-}$; AMPKα2$^{F/F}$ embryos at E15 using plasmids expressing EGFP (Fig. 2 *A* and *A′*) or Cre recombinase-internal ribosome entry site (IRES)-EGFP (Fig. 2 *B* and *B′*) to simultaneously visualize neuronal morphology and achieve Cre-mediated recombination of AMPKα2. Following organotypic slice culture for 5 d ex vivo (DEV), this technique allows monitoring of both neuronal migration and axon formation of cortical progenitors from the ventricular zone (VZ) to their final position in the cortical plate (CP) (15, 18). Because the progenitors electroporated at E15 give rise primarily to callosally projecting pyramidal neurons destined to layer 2–3, most axons emerging from GFP-expressing

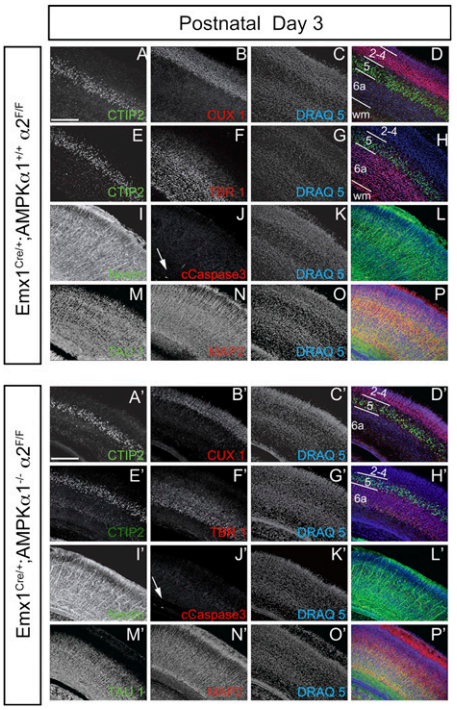

Fig. 1. AMPKα is not required for cortical neuron development in vivo. Immunohistochemical analysis of AMPKα-DcKO (Emx1$^{Cre/+}$; AMPKα1$^{-/-}$; AMPKα2$^{F/F}$) mice and control (Emx1$^{Cre/+}$; AMPKα1$^{+/+}$; AMPKα2$^{F/F}$) littermates P3 brain slices using layer 2–4 marker Cux1 (*A*, *A′*, *E*, and *E′*), layer 5 marker CTIP2 (*B* and *B′*), layer 6a marker Tbr1 (*F* and *F′*), radial glial progenitor marker nestin (*I* and *I′*) and apoptotic marker cleaved caspase 3 (*J* and *J′*), axonal marker Tau1 (*M* and *M′*), dendritic marker MAP2 (*N* and *N′*) and DRAQ5 nuclear marker shows cytoarchitecture (*C*, *C′*, *G*, *G′*, *K*, *K′*, *O*, and *O′*). Arrows in *J* and *J′* point to a cleaved caspase 3-positive cell body. Data are representative of four independent knockout analyses for each genotype. (Scale bar, 150 μm.)

neurons (red arrow in Fig. 2*A*) project toward the midline (arrowheads in Fig. 2 *A* and *A′*) in control mice (AMPKα1$^{-/-}$; AMPKα2$^{F/F}$ electroporated with EGFP only). The same numbers of axons are projecting toward the midline in AMPKα-DcKO neurons (AMPKα1$^{-/-}$; AMPKα2$^{F/F}$ electroporated with Cre-IRES-EGFP plasmid) (red arrow in Fig. 2*B*). We also found no difference in the distribution of neurons in control and AMPKα-DcKO slices (Fig. S2) confirming our layer-specific marker analysis, which suggests that AMPK catalytic activity is not required for neurogenesis or neuronal migration.

Optical isolation of single neurons using confocal microscopy revealed that control neurons migrating through the intermediate zone (IZ) display a thick leading process (LP; arrows in Fig. 2*C*) and a long trailing process (TP; arrowhead in Fig. 2*C*) that become the apical dendrite and the axon, respectively, in postmigratory neurons that reached the CP (15, 21, 22). We did not observe any qualitative difference in LP/apical dendrite and TP/axon formation in AMPKα-DcKO neurons (AMPKα1$^{-/-}$; AMPKα2$^{F/F}$ electroporated with Cre-IRES-EGFP plasmid) (Fig. 2*D*) compared with control neurons (Fig. 2*C*). Quantifying the percentage of neurons displaying a single TP/axon or either no axon or multiple axons confirmed that AMPKα-DcKO neurons show no axon specification defect compared with control neurons (Fig. 2*E*).

We also used an independent method to assess axon formation by performing EUCE coupled with immediate dissociation and in vitro culture for 5 div. This method allows pyramidal neurons to polarize in vitro and subsequent analysis with single cell resolution revealed that axons (labeled by Tau1) and dendrites (labeled with MAP2) (Fig. S3 *A*–*D′*) polarize normally in AMPKα-DcKO neurons (Fig. 2*G*) compared with control neurons (Fig. 2*F*). Finally, we used a pharmacological approach to inhibit AMPK

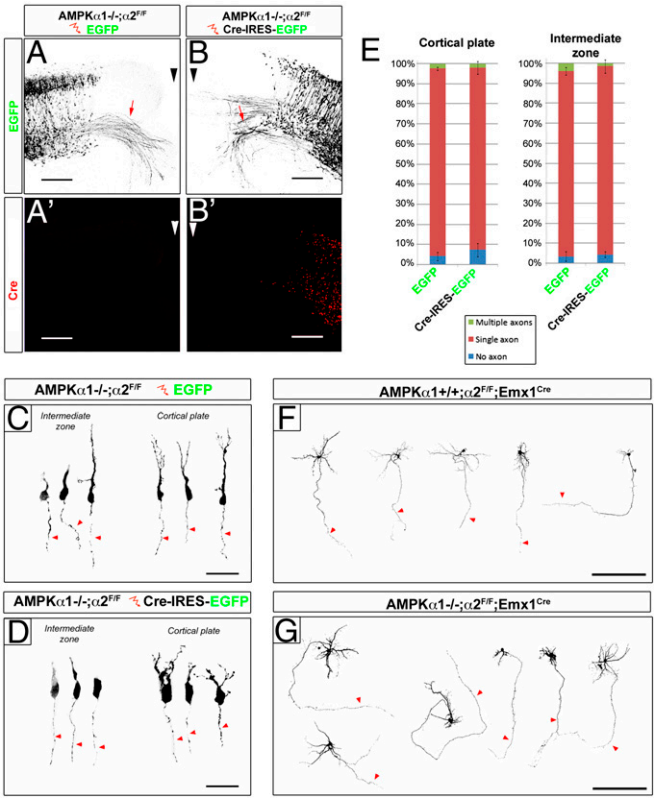

Fig. 2. Axon formation is not impaired in AMPK-deficient cortical neurons. (*A*–*B*′) The cortex of E15.5 AMPKα1$^{-/-}$; AMPKα2$^{F/F}$ embryos were electroporated with EGFP alone (*A* and *A*′) or Cre-IRES-EGFP expressing vectors (*B* and *B*′) and then maintained for 5 DEV in organotypic slice culture. Axon projections (arrows) toward the midline (arrowheads) are identical in AMPKα-deficient and control neurons. (Scale bar, 150 μm.) (*C* and *D*) Optically isolated EGFP-labeled neurons in control EGFP-expressing neurons (*C*) or Cre-IRES-EGFP–expressing neurons (*D*) in the IZ or CP of slice shown in *A*–*B*′ reveal no morphological defects in AMPK-deficient neurons compared with control. Arrows point to LP/apical dendrite and arrowheads to TP/axon. (Scale bar, 10 μm.) (*E*) Quantitative morphological analysis of single neurons reveals that more than 90% of the electroporated cells display a single TP/axon in control (EGFP only) and AMPK-deficient (Cre-IRES-EGFP) neurons both in the CP and IZ. Graphs represent mean percentages of three independent experiments. Error bars represent SE to the mean (SEM). (*F* and *G*) Morphology of cortical neurons electroporated with EGFP-expressing vector isolated from Emx1$^{Cre/+}$; AMPKα1$^{+/+}$; AMPKα2$^{F/F}$ (*F*) or Emx1$^{Cre/+}$; AMPKα1$^{-/-}$; AMPKα2$^{F/F}$ (*G*) E15 embryos. Neurons were maintained in dissociated culture for 16 div. AMPK-deficient neurons (*G*) do not display any polarity defect compared with control neurons still expressing one isoform of AMPK (*F*). Arrowhead points to the axon. (Scale bar, 300 μm.)

catalytic activity by incubating cortical neurons in vitro with compound C, a nonselective but potent AMPK inhibitor (Fig. S4 *B* and *E*). Qualitative and quantitative assessments demonstrate that compound C does not affect cortical neuron differentiation (Fig. S4 *B* and *E*) compared with control neurons exposed to vehicle only (DMSO; Fig. S4 *A* and *E*). Overall, our genetic and pharmacological approaches demonstrate that AMPK catalytic activity is not required for proper neurogenesis, neuronal migration, polarization, or survival in vivo or in vitro.

Metabolic Stress Impairs Axogenesis in Cortical Neurons. AMPK is an important metabolic sensor required to maintain epithelial cell polarity during metabolic stress such as nutrient deprivation and lowering of the ATP:AMP ratio (6, 9). We wanted to test whether various forms of metabolic stress known to activate AMPK, including exposure to the mitochondrial inhibitor metformin—the drug most prescribed to treat type 2 diabetes—or the stimulator of glucose uptake, AICAR, would affect neuronal polarization. As expected, we show that metformin and AICAR (Fig. S5) robustly activate AMPK in neurons by measuring the levels of active phospho-AMPKα and the phosphorylation of its downstream targets ACC and $GABA_B$ R2 after treatment. Interestingly, treatments of E15 cortical neurons for 4 div with either metformin or AICAR showed a dose-dependent effect on neuronal polarization leading to over 85% of neurons without a Tau1 positive axon (Fig. S3 *E*–*L* and Fig. S4 *C*, *D*, *F*, and *G*). Importantly, because >95% of cells electroporated by EUCE are radial glial progenitors (18), these results confirm that generic steps of neuronal differentiation are not affected by these treatments because over 90% of the cells express panneuronal markers including Tau1 and MAP2 (Figs. S3 and S4). However, in the presence of metformin or AICAR, these neurons fail to polarize properly. Specifically, neurons fail to form a single Tau1-positive (MAP2-negative) axon, but instead have multiple short neurites aberrantly labeled by both Tau1 and MAP2 (Fig. S3). These results demonstrate that axon formation is highly sensitive to metabolic stress. We next tested whether these effects are mediated through AMPK activation during neuronal polarization.

Axonal Effects of AICAR, but Not Metformin, Require AMPK. Recent studies have reported that some of the effects of metformin are AMPK independent (23). We therefore tested whether the effects of AICAR and metformin on axon specification and elongation were mediated through AMPK by exposing either control or AMPKα-DcKO cortical neurons to AICAR or metformin in vitro (Fig. 3). Both metformin (Fig. 3 *E*–*H* and *M*) and AICAR (Fig. 3 *I*–*L* and *N*) treatments significantly reduced the percentage of cortical neurons successfully polarizing compared with control (Fig. 3 *A*–*D*, *M*, and *N*). Surprisingly, the effects of metformin were only partially mediated by AMPK activation because AMPKα-deficient cortical neurons still show a significantly higher proportion of neurons without Tau1-postive axon compared with control (Fig. 3 *E*′–*H*′ and *M*). This is in sharp contrast with AMPKα-deficient cortical neurons exposed to AICAR, which show similar proportion of neurons correctly polarized with a single axon compared with controls (Fig. 3 *I*′–*L*′ and *N*).

Interestingly, when we quantified the effects of metformin and AICAR on the axon length for neurons that successfully polarized, the dependence on AMPK was even more divergent (Fig. 3*O*). We found that axon length of AMPKα-DcKO cortical neurons treated with metformin were not significantly longer than wild-type neurons treated with metformin. Conversely, AMPKα-deficient cortical neurons treated with AICAR exhibited axon length significantly longer than wild-type neurons treated with AICAR yet indistinguishable from vehicle-treated WT neurons cultured in the same conditions. Overall, these results demonstrate that unlike AICAR, which mediates its effects on axon specification and outgrowth almost exclusively through AMPK activation, metformin mediates some of its effects on neuronal polarization and extension in an AMPK-independent manner consistent with metformin AMPK-independent effects documented by others in nonneuronal cell types (24, 25).

AMPK Overactivation Inhibits Axon Formation Through Inhibition of the mTOR Pathway. We next determined the molecular mechanisms underlying the inhibition of axon formation mediated by AMPK overactivation. Several downstream effectors have been shown to mediate the effect of AMPK on cell polarity in different organisms ranging from actomyosin effectors such as the activating phosphorylation of myosin light chain (MLC) (26) to the mTOR pathway (27, 28). Interestingly, both MLC phosphorylation/myosin-II activity (29) and TSC1/2-dependent mTOR inactivation (30) have been implicated in neuronal polarization and axon formation. Paradoxically treatment with metformin and AICAR did not increase the level of MLC phosphorylation on Ser19 in cortical neurons. We therefore focused on testing the function of the mTOR kinase pathway, which is a key regulator of protein synthesis through the mTORC1 complex. AMPK has been shown to directly phosphorylate TSC2 (27), an essential

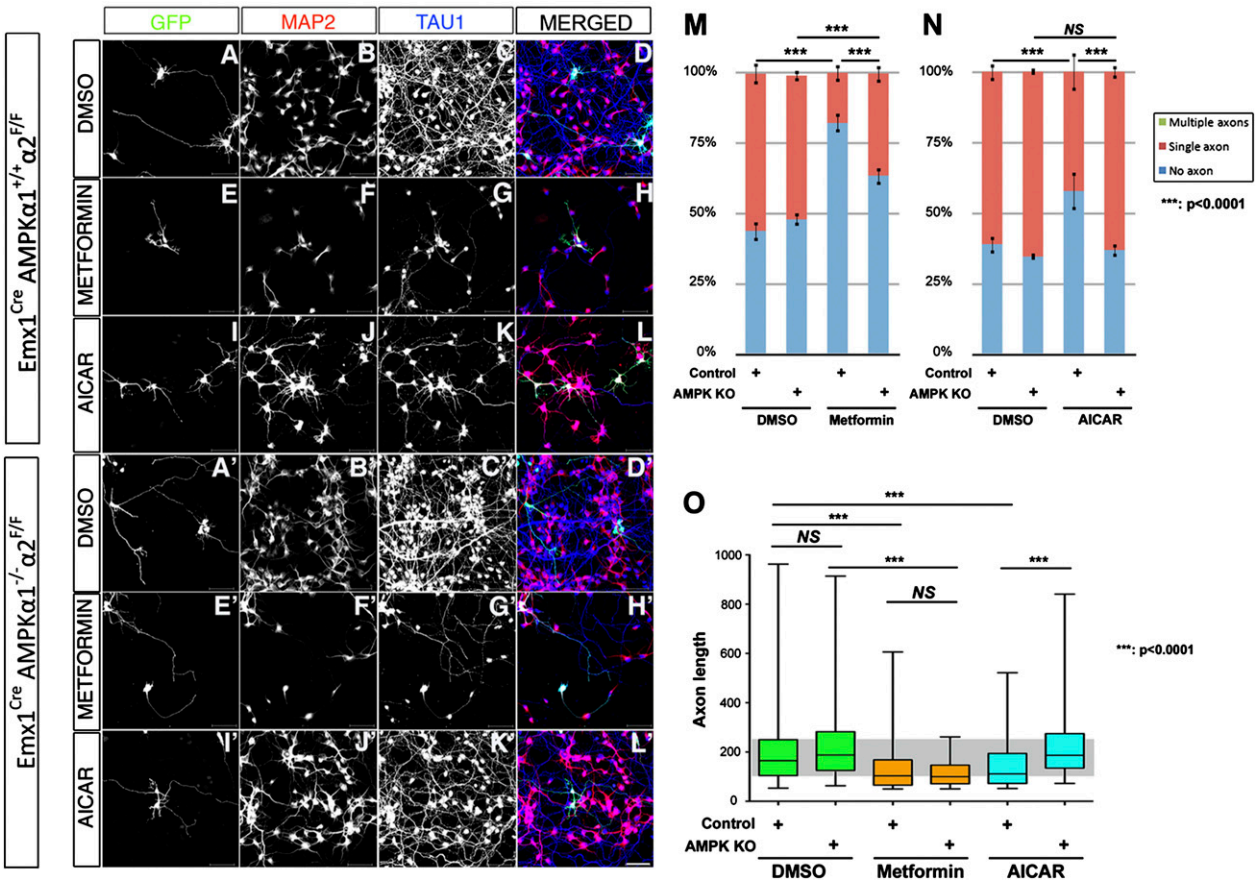

Fig. 3. Effects of AICAR but not metformin on axon specification and outgrowth are entirely mediated by AMPK. (*A–L′*) Cortical neurons from control ($Emx1^{Cre/+}$; $AMPK\alpha1^{+/+}$; $AMPK\alpha2^{F/F}$; *A–L*) or AMPKα-DcKO ($Emx1^{Cre/+}$; $AMPK\alpha1^{-/-}$; $AMPK\alpha2^{F/F}$; *A′–L′*) animals were electroporated and dissociated at E15.5. After 2 div, neurons were treated with either vehicle (DMSO, *A/A′–D/D′*), metformin (1 mM, *E/E′–H/H′*), or AICAR (1 mM, *I/I′–L/L′*) for 3 div. After fixation, cultures were stained for EGFP, Tau1 (blue), and MAP2 (red). (*M* and *N*) Neuronal polarity was quantified for three independent experiments (≥300 neurons for each treatment) for neurons from control animals or AMPKα-DcKO. (*O*) Axon length was measured using ImageJ software. Box plots representing the 10th, 25th, median, 75th, and 90th percentiles illustrate the distribution of the data. Fisher's exact test was used to statistically analyze the data represented in *A/A′–L/L′*. Statistical analysis conducted on axon length was performed using one-way ANOVA.

component of the tuberin/hamartin complex that also contains the protein TSC1. Activation of the TSC1/TSC2 complex by AMPK enhances its inhibitory GAP activity toward Rheb GTPase, an activator of mTOR. AMPK also exerts a second brake on the mTOR pathway by phosphorylating raptor, a phosphorylation that inhibits the activity of the complex and thereby inhibits protein synthesis. Treatment of cortical neurons in vitro with metformin (Fig. S6) and AICAR (Fig. 4 *A* and *B*) significantly increased the phosphorylation of AMPK (phospho-Thr172) and raptor (phospho-Ser792), whereas mTOR (phospho-Ser2448) and p70S6K (phospho-Ser371) phosphorylation was decreased. Both treatments also resulted in the disappearance of a slow migrating band corresponding to the hyperphosphorylated form of protein 4E-BP1 (arrow in Fig. 4*A*) with increases in a faster migrating, hypophosphorylated band. These results are compatible with previous studies and demonstrate that in cortical neurons, AMPK activation inhibits the mTOR pathway. Because TSC1/2 regulates neuronal polarization by inhibiting axon formation (30), we tested whether AMPK overactivation inhibits axon formation through excessive TSC1/2-mediated inhibition of mTOR. To do this, we performed independent TSC1 and TSC2 knockdown in the presence of AICAR. We confirmed that knockdown of TSC2 leads to a significant increase in neurons bearing multiple axons (Fig. 4 *C–F*) as previously published (30). Most interestingly, knockdown of TSC1 and TSC2 completely rescued the effect of AICAR treatment on axon formation (Fig. 4 C′–E′ and *F*) and axon growth (Fig. 4*G*). These results strongly argue that AMPK overactivation inhibits axon specification and axon growth by activating TSC1/2 and thereby inhibiting mTOR.

Discussion

Our results demonstrate unequivocally that AMPK catalytic activity is not required for proper cortical neurogenesis, radial migration, cortical layer formation, and axon–dendrite formation in vivo and in vitro. Neuronal survival in the developing cortex is also not affected by the genetic removal of all AMPKα. Our results are in conflict with a prior study, which suggested that AMPK is required for embryonic cortical development including neurogenesis, neuronal survival, and differentiation (10). To date, the large body of work suggests a dogma whereby the AMPKβ subunit is an obligate trimer with AMPKα and AMPKγ with effects mediated by the catalytic activity of AMPKα (5).

In part, this apparent discrepancy might be due to the nature of the genetic allele used in the prior study. This prior study (10) used a gene-trap allele of the regulatory subunit AMPKβ1, which expresses a hybrid protein made of the first 224 (out of 270) amino acids of AMPKβ1 fused in its C-terminal to β-galactosidase that could generate a protein with altered function rather than representing an AMPKβ1-null mouse model. It may be possible that the expression of a foreign fusion protein with a myristoylation signal (from AMPKβ1) could impair cellular function and induce a type of nonphysiological stress that unmasks an AMPK-dependent function. Another more straightforward possibility is that AMPKβ1 simply has independent

functions of AMPKα despite the current dogma. Future investigation of the proteins that AMPKβ1 binds to and regulates might resolve this discrepancy. However, a second group (31), which recently globally disrupted AMPKβ1 by conventional loss-of-function gene targeting, failed to find neuronal development phenotypes and obtained viable and fertile AMPKβ1-knockout mice. Currently, AMPKα is largely thought to mediate AMPK catalytic activity and therefore our genetic loss-of-function data likely reflect the role of AMPK activity in the developing nervous system. Our results also reveal different phenotypes from LKB1 loss-of-function mutants in the same neurons, which require LKB1 for neuronal polarization and survival in vivo (15, 16). In other model organisms, including *Drosophila*, LKB1 neural phenotypes are always significantly more severe than AMPKα phenotypes (32), which could be due to the fact that LKB1 is upstream of AMPK and at least 11 other kinases (33, 34). Our results are consistent with such studies and we speculate that during mammalian embryonic brain development AMPKα activity is present but not essential for proper neural development; however, its hyperactivation has profound consequences on early neural development. This is largely compatible with data from other multicellular organisms like *Caenorhabditis elegans* where AMPKα is not required for normal development, but only for surviving energetic stress paradigms (35). Our results are also consistent with genetically null AMPKα *Drosophila* mutants that specify neurons in the embryo and adult properly, which extend axons and dendrites (6, 33).

The mTOR-dependent pathway has previously been involved in neuronal polarization, when TSC1/2 inhibits axon specification by repressing SAD-A/B kinases protein synthesis (29). Importantly, our study shows that the inhibitory effects on axon formation and growth via AMPK overactivation require TSC1 and -2. Knockdown of TSC1 and TSC2 results in full rescue of axon formation and axon growth during AICAR-induced AMPK activation (Fig. S7*A*).

We have previously shown that, unlike in other cell types (2), LKB1 is not the major AMPK-activating kinase in neurons because there is no significant change in T172 phosphorylation in LKB1-deficient neurons in vivo (15). Ca^{2+}-calmodulin–dependent kinase kinase β (CAMKKβ) has previously been shown to phosphorylate T172 on AMPK in neurons and might therefore be the relevant upstream activator of AMPK in neurons (36) (Fig. S7*A*).

Our results show that axogenesis and axon growth can be impaired during times of severe energetic stress, which potently activates AMPK (1, 2, 6) (Fig. S7*B*). We were able to show in vitro that cultured cortical neurons treated with AICAR or metformin lead to aberrant neuronal polarization. Future investigations

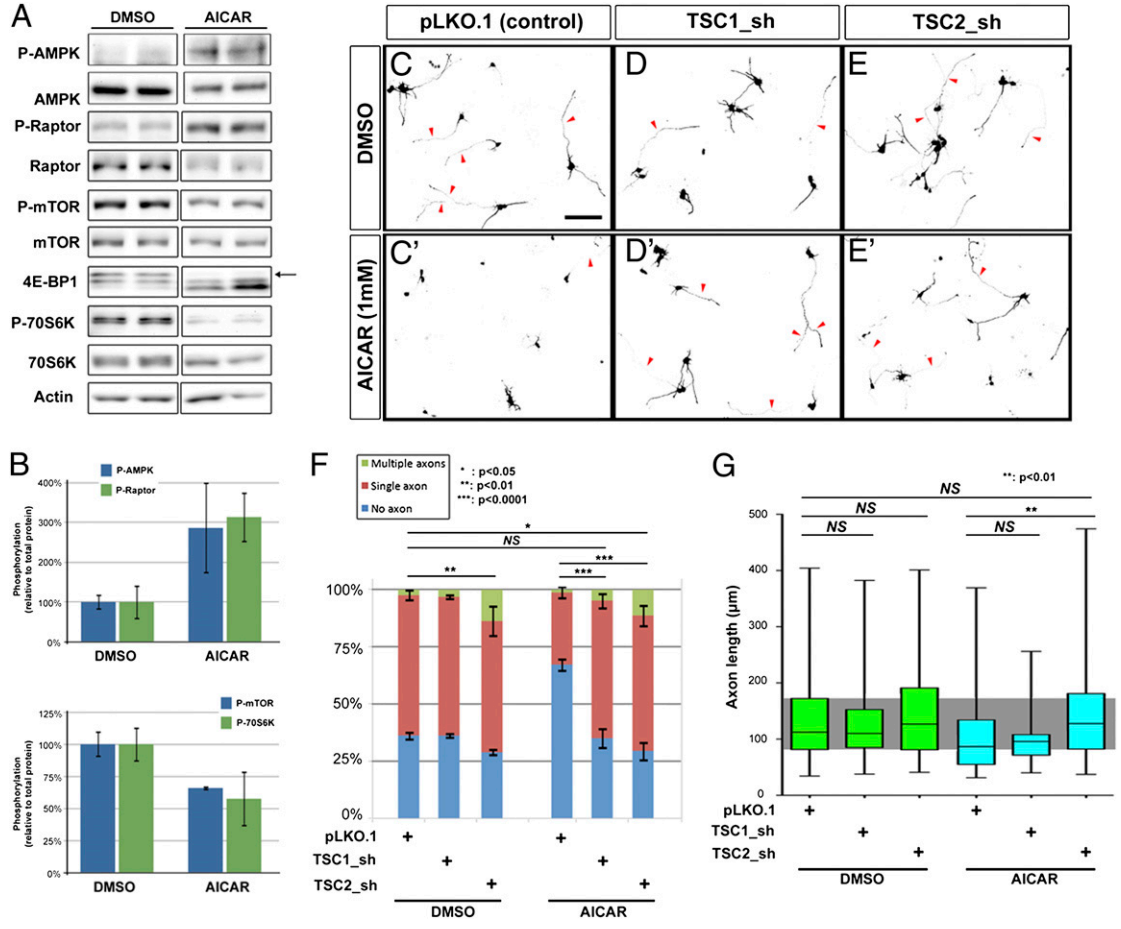

Fig. 4. AMPK activation impairs axon formation through the TSC/mTOR pathway. (*A*) Western blot analysis after in vitro culture of E18.5 mouse cortical neurons cultured for 1 d, then treated with AICAR (1 mM) for 3 d in vitro. Treatments increased the phosphorylation of AMPK (phospho-Thr172) and raptor (phospho-Ser792), whereas mTOR (phospho-Ser2448) and p70S6K (phospho-Ser371) phosphorylation were decreased. Treatment also resulted in the disappearance of a slow migrating band corresponding to 4E-BP1 (arrow). (*B*) Quantification of phospho-AMPK, phospho-raptor, phospho-mTOR, and phospho-70S6K signal normalized to total amount of corresponding proteins compared with control condition (DMSO vehicle only). Error bars represent SEM ($n = 5$). (*C–E*) Morphology of cortical neurons electroporated with control vector (*C*), or short-hairpin (sh)RNA targeting TSC1 (*D*), or TSC2 (*E*) and cultured in vitro for 4 d exposed to control vehicle only (DMSO) or the AMPK activator AICAR (1 mM). Arrowheads point to single axons. (Scale bar, 100 μm.) (*F*) Neuronal polarity was quantified by determining the percentage of neurons with single axon, multiple axons, or no axon for five independent experiments (≥500 neurons for each treatment) for neurons shown in *C–E*. Statistical analyses were performed using Fisher's exact test. (*G*) Quantification of axon length for neurons shown in *C–E*. Box plots are as in Fig. 3. Statistical analysis was performed using one-way ANOVA.

should determine whether metabolic stress, environmental insults, or other pathological situations known to activate AMPK, could impact brain development through its ability to modulate axon formation, axon growth, and maybe other aspects of neuronal differentiation. Our results have important implications in the context of neurodegeneration especially in light of recent results suggesting that in *Drosophila*, neurodegeneration induced by Par1 (MARK)-mediated Tau-hyperphosphorylation can be significantly suppressed by reducing LKB1 expression (37, 38). Future experiments should further explore the relationship between metabolic stress, AMPK activation, and axon formation, growth, or maintenance in the context of neurodegeneration.

Materials and Methods

Animals. Mice were used according to protocols approved by the Institutional Animal Care and Use Committee at the University of North Carolina-Chapel Hill, The Scripps Research Institute, and in accordance with National Institutes of Health guidelines. Time-pregnant females were maintained in a 12 h light/dark cycle and obtained by overnight breeding with males of the same strain. Noon following breeding is considered as E0.5.

Antibodies. See Table S1.

Constructs and Reagents. All cDNAs were subcloned into a pCIG2 vector (18), which contains a (cDNA)-IRES-EGFP under the control of a CMV-enhancer/chicken β-actin promoter. pCIG2:CRE has been described previously (18). shRNA vectors targeting mouse Tsc1 and Tsc2 genes were selected from the TRC library and purchased from Sigma-Aldrich. All chemicals were purchased from Sigma excepted when indicated otherwise. Neurons were treated with the following drugs: In solution AMPK inhibitor compound C (Calbiochem), AICAR (Toronto Research Chemicals), and metformin (Sigma). The treatments were performed by adding the drug at the concentration indicated in figure legends directly in the culture medium. AMPK activation/inhibition was maintained over several days by adding to the culture medium half of the indicated concentration every day.

RT and PCR. mRNA from mouse cortex were obtained by RNA extraction and purification using Nucleospin RNA II kit (Macherey Nagel). RNA was treated with DNase I during the purification procedure to prevent contamination of the samples with genomic DNA, as recommended by the manufacturer. cDNA conversion was performed with Qiagen Omniscript kit using 1 μg mRNA as template and oligodT primers (Invitrogen). Fragments specific to AMPK α1, α2, and GAPDH were obtained using the following primers: PRKAA1_F 5′-GCTGTGGCTCACCCAATTAT-3′ and PRKAA1_R 5′-TGTTGTACAGGCAGCTGAGG-3′, PRKAA2_F 5′-CGCCTCTAGTCCTCCATCAG-3′ and PRKAA2_R 5′-CAGCTGTGCTGGAATCAAAA-3′, and GAPDH_F 5′-AACTTTGGCATTGTGGAAGG-3′ and GAPDH_R 5′-CCCTGTTGCTGTAGCCGTAT-3′. Thirty cycles of PCR were performed using Taq DNA polymerase (Qiagen) at the hybridization temperature of 57.5 °C.

Western Blotting. Western blotting was performed as described previously (18). See *SI Materials and Methods* for details.

Ex Utero Electroporation and Organotypic Slice Culture. EUCE was performed as described previously (18) (*SI Materials and Methods*).

ACKNOWLEDGMENTS. We thank the members of the J.E.B. and F.P. laboratories for helpful comments. This work was supported by National Institutes of Health grants (R01MH073155 to J.E.B. and T.W., and R01AG031524 to F.P. and J.C.), University Funds for J.E.B., and a postdoctoral fellowship from the Fondation pour la Recherche Médicale and the Philippe Foundation (to J.C.).

1. Hardie DG, Carling D, Carlson M (1998) The AMP-activated/SNF1 protein kinase subfamily: Metabolic sensors of the eukaryotic cell? *Annu Rev Biochem* 67:821–855.
2. Shaw RJ, et al. (2004) The tumor suppressor LKB1 kinase directly activates AMP-activated kinase and regulates apoptosis in response to energy stress. *Proc Natl Acad Sci USA* 101:3329–3335.
3. Stapleton D, et al. (1996) Mammalian AMP-activated protein kinase subfamily. *J Biol Chem* 271:611–614.
4. Concannon CG, et al. (2010) AMP kinase-mediated activation of the BH3-only protein Bim couples energy depletion to stress-induced apoptosis. *J Cell Biol* 189:83–94.
5. Hardie DG (2004) The AMP-activated protein kinase pathway—new players upstream and downstream. *J Cell Sci* 117:5479–5487.
6. Mirouse V, Swick LL, Kazgan N, St Johnston D, Brenman JE (2007) LKB1 and AMPK maintain epithelial cell polarity under energetic stress. *J Cell Biol* 177:387–392.
7. Nakano A, et al. (2010) AMPK controls the speed of microtubule polymerization and directional cell migration through CLIP-170 phosphorylation. *Nat Cell Biol* 12:583–590.
8. Poels J, Spasic MR, Callaerts P, Norga KK (2009) Expanding roles for AMP-activated protein kinase in neuronal survival and autophagy. *Bioessays* 31:944–952.
9. Williams T, Brenman JE (2008) LKB1 and AMPK in cell polarity and division. *Trends Cell Biol* 18:193–198.
10. Dasgupta B, Milbrandt J (2009) AMP-activated protein kinase phosphorylates retinoblastoma protein to control mammalian brain development. *Dev Cell* 16:256–270.
11. Viollet B, et al. (2003) Physiological role of AMP-activated protein kinase (AMPK): Insights from knockout mouse models. *Biochem Soc Trans* 31:216–219.
12. Andreelli F, et al. (2006) Liver adenosine monophosphate-activated kinase-alpha2 catalytic subunit is a key target for the control of hepatic glucose production by adiponectin and leptin but not insulin. *Endocrinology* 147:2432–2441.
13. Jorgensen SB, et al. (2004) Knockout of the alpha2 but not alpha1 5′-AMP-activated protein kinase isoform abolishes 5-aminoimidazole-4-carboxamide-1-beta-4-ribofuranosidebut not contraction-induced glucose uptake in skeletal muscle. *J Biol Chem* 279:1070–1079.
14. Gorski JA, et al. (2002) Cortical excitatory neurons and glia, but not GABAergic neurons, are produced in the Emx1-expressing lineage. *J Neurosci* 22:6309–6314.
15. Barnes AP, et al. (2007) LKB1 and SAD kinases define a pathway required for the polarization of cortical neurons. *Cell* 129:549–563.
16. Shelly M, Cancedda L, Heilshorn S, Sumbre G, Poo MM (2007) LKB1/STRAD promotes axon initiation during neuronal polarization. *Cell* 129:565–577.
17. Bortone D, Polleux F (2009) KCC2 expression promotes the termination of cortical interneuron migration in a voltage-sensitive calcium-dependent manner. *Neuron* 62:53–71.
18. Hand R, et al. (2005) Phosphorylation of Neurogenin2 specifies the migration properties and the dendritic morphology of pyramidal neurons in the neocortex. *Neuron* 48:45–62.
19. Kuramoto N, et al. (2007) Phospho-dependent functional modulation of GABA(B) receptors by the metabolic sensor AMP-dependent protein kinase. *Neuron* 53:233–247.
20. Kishi M, Pan YA, Crump JG, Sanes JR (2005) Mammalian SAD kinases are required for neuronal polarization. *Science* 307:929–932.
21. Kriegstein AR, Noctor SC (2004) Patterns of neuronal migration in the embryonic cortex. *Trends Neurosci* 27:392–399.
22. Noctor SC, Martinez-Cerdeno V, Ivic L, Kriegstein AR (2004) Cortical neurons arise in symmetric and asymmetric division zones and migrate through specific phases. *Nat Neurosci* 7:136–144.
23. Kalender A, et al. (2010) Metformin, independent of AMPK, inhibits mTORC1 in a rag GTPase-dependent manner. *Cell Metab* 11:390–401.
24. Foretz M, et al. (2010) Metformin inhibits hepatic gluconeogenesis in mice independently of the LKB1/AMPK pathway via a decrease in hepatic energy state. *J Clin Invest* 120:2355–2369.
25. Miller RA, Birnbaum MJ (2010) An energetic tale of AMPK-independent effects of metformin. *J Clin Invest* 120:2267–2270.
26. Lee JH, et al. (2007) Energy-dependent regulation of cell structure by AMP-activated protein kinase. *Nature* 447:1017–1020.
27. Gwinn DM, et al. (2008) AMPK phosphorylation of raptor mediates a metabolic checkpoint. *Mol Cell* 30:214–226.
28. Inoki K, Zhu T, Guan KL (2003) TSC2 mediates cellular energy response to control cell growth and survival. *Cell* 115:577–590.
29. Kollins KM, Hu J, Bridgman PC, Huang YQ, Gallo G (2009) Myosin-II negatively regulates minor process extension and the temporal development of neuronal polarity. *Dev Neurobiol* 69:279–298.
30. Choi YJ, et al. (2008) Tuberous sclerosis complex proteins control axon formation. *Genes Dev* 22:2485–2495.
31. Dzamko N, et al. (2010) AMPK beta1 deletion reduces appetite, preventing obesity and hepatic insulin resistance. *J Biol Chem* 285:115–122.
32. Amin N, et al. (2009) LKB1 regulates polarity remodeling and adherens junction formation in the Drosophila eye. *Proc Natl Acad Sci USA* 106:8941–8946.
33. Alessi DR, Sakamoto K, Bayascas JR (2006) LKB1-dependent signaling pathways. *Annu Rev Biochem* 75:137–163.
34. Lizcano JM, et al. (2004) LKB1 is a master kinase that activates 13 kinases of the AMPK subfamily, including MARK/PAR-1. *EMBO J* 23:833–843.
35. Narbonne P, Roy R (2009) Caenorhabditis elegans dauers need LKB1/AMPK to ration lipid reserves and ensure long-term survival. *Nature* 457:210–214.
36. Anderson KA, et al. (2008) Hypothalamic CaMKK2 contributes to the regulation of energy balance. *Cell Metab* 7:377–388.
37. Nishimura I, Yang Y, Lu B (2004) PAR-1 kinase plays an initiator role in a temporally ordered phosphorylation process that confers tau toxicity in Drosophila. *Cell* 116:671–682.
38. Wang JW, Imai Y, Lu B (2007) Activation of PAR-1 kinase and stimulation of tau phosphorylation by diverse signals require the tumor suppressor protein LKB1. *J Neurosci* 27:574–581.

Supporting Information

Williams et al. 10.1073/pnas.1013660108

SI Materials and Methods

Ex Utero Electroporation and Organotypic Slice Culture. Briefly, a solution containing 1 μg/μL of endotoxin-free plasmid DNA and 0.5% Fast Green as a loading dye (Sigma; 1:20 ratio) was microinjected into the lateral ventricles of isolated E15.5 embryonic mouse heads that were decapitated and placed in complete HBSS medium [1× HBSS solution (Gibco), 2.5 mM Hepes pH 7.4, 30 mM D-glucose, 1 mM $CaCl_2$, 1 mM $MgSO_4$, 4 mM NaHCO3]. Plasmid DNA was then introduced into radio-glial telencephalic progenitors of the ventricular zone by electroporation with gold-coated electrodes using an ECM 830 electroporator (BTX) and the following parameters: five 100-ms long pulses separated by 100-ms long intervals at 30 V. For slice culture, the brain was extracted immediately after electroporation, embedded in 3% low-melting agarose, and vibratome sectioned (250-μm thick sections) using a Leica VT1000S vibratome. The resulting slices were cultured organotypically for 5 d using an air interface protocol on transwell inserts (1-μg pore size) coated with poly-D lysine (83 mg/mL; Sigma) and laminin (8.3 mg/mL), then fixed with 4% paraformaldehyde and stained for immunofluorescence. Dissociated E15.5 cortical cultures were performed using a papain-based enzymatic dissociation method as previously described. A total of 1.25×10^5 dissociated cortical progenitors were plated on 12-mm glass coverslips coated with laminin and poly-L lysine and cultured in serum-free culture medium (NeuroBasal medium supplemented with L-glutamine and penicillin/streptomycin, plus B27 and N2 supplements). Neuronal cultures were ultimately fixed with 4% paraformaldehyde and stained for immunofluorescence.

Western Blotting. Cells were scraped via cell lifter (Corning), harvested in culture medium, and centrifuged at 1,000 RPM for 5 min. Pellet was washed two times in cold DPBS and lysed in ice-cold lysis buffer containing 25 mM Tris (pH7.5), 2 mM $MgCl_2$, 600 mM NaCl, 2 mM EDTA, 0.5% Nonidet P-40, and 1× protease and phosphatase mixture inhibitors (Sigma). Aliquots of the proteins were separated on 4–12% NuPAGE BisTris and then transferred to a polyvinylidene difluoride (PVDF) membrane. After transfer, the membrane was washed three times in TBS, blocked for 1 h at room temperature in 5% BSA in TBS, followed by 4 °C overnight incubation with appropriate primary antibody in 5% BSA-TBS. Western blot analysis was performed at 1:1,000 dilution of all primary antibodies with the following exception: anti-α tubulin (1:15,000). Next day, the membrane was washed three times in TBS-Tween, incubated at room temperature for 1 h with IRDye infrared secondary antibody (LI-COR Biosciences) at 1:2,000 dilution in 5% BSA-TBS, followed by 2× TBS-T and 1× TBS washes. Scanning, analyzing, and quantification of blots were performed via the Odyssey Infrared Imaging System (Fig. S1 *D–G*) or Alpha Innotech FluorChemQ (all others). Three or more independent experiments were performed for all immunoblotting data. Quantification data are represented by bar graphs with error bars that indicate the SEM.

Constructs and Reagents. The following vectors were used (percentages indicate the knockdown level indicated by Sigma-Aldrich for validated shRNA vectors, when the information is available): TRCN0000113949 (70%) and TRCN0000113950 for Tsc1 and TRCN0000042723 (71%) and TRCN0000042724 (91%) for Tsc2. For each gene, shRNA coding plasmids were pooled to a final concentration of 1 μg/μL (1:1 ratio) and co-transfected with GFP-coding pCIG2 vector (0.5 μg/μL final concentration).

Immunofluorescent Staining. Dissociated neuronal cultures and organotypic slice cultures were fixed with 4% paraformaldehyde for 30 min. Postnatal mouse brains were fixed by intracardiac perfusion of 4% paraformaldehyde after anesthesia with avertin. Following perfusion, brains were quickly dissected and postfixed in 4% paraformaldehyde for 60 min, then sectioned (50-μm thick sections) as described above. Following fixation, samples were washed with PBS three times and then permeabilized in blocking buffer (1× PBS, 5% BSA, 0.05% Triton X-100) for 1 h. Incubation with primary antibodies was performed overnight with the indicated antibodies diluted in blocking buffer supplemented with 10% goat serum. After three washes with 1× PBS, the samples were stained with the appropriate Alexa conjugated secondary antibodies (Molecular Probes; 1:2,000) for 1 h. Cells were then washed in PBS and slides were mounted. Nuclear DNA was stained with DRAQ5 dye (Alexis; 1:10,000). Fluorescent immunostaining was observed using a LEICA TCS-SL laser scanning confocal microscope equipped with an Argon laser (488 nm), green Helium-Neon laser (546 nm), and red Helium-Neon laser (633 nm) for observation of Alexa-488/GFP, Alexa-546, and Alexa-647/DRAQ5, respectively.

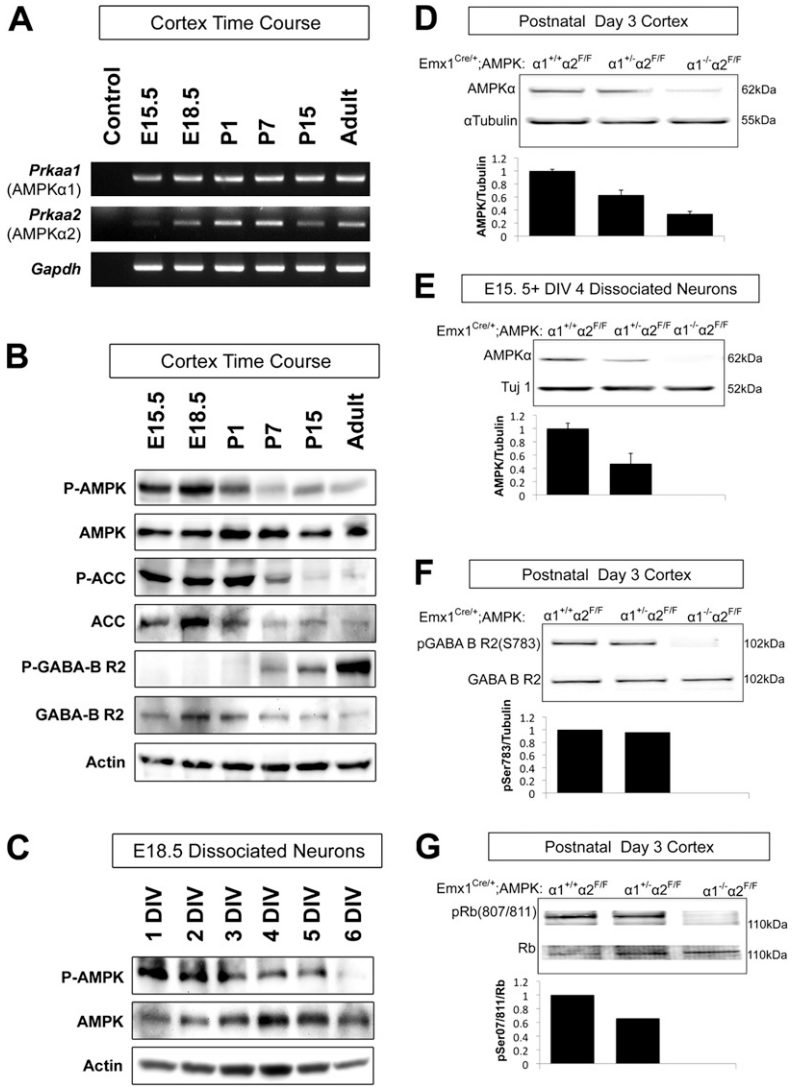

Fig. S1. Expression of AMPKα1 and AMPKα2 in the developing cortex. (*A*) Expression profile of AMPKα1 and AMPKα2 at various developmental stages. RT-PCR on total mRNA extracted from mouse cortex. The housekeeping mRNA Gapdh was used as an internal control. The control lane represents a RT-PCR performed with no template RNA. (*B*) Expression and activity of AMPKα proteins in the mouse cortex. The catalytic activity of the AMPK enzyme was determined by the phosphorylation of AMPKα on threonine 172 residue (p-AMPK), and by the phosphorylation of its downstream targets ACC and $GABA_B$ R2. Actin expression was used for normalization. (*C*) Expression and activity of AMPKα proteins in cortical neurons cultured in vitro. Cortical neurons were grown in vitro after dissociation in conditions allowing their progressive polarization, and collected every day. Western blot analysis was performed to monitor the expression level of total and phosphorylated AMPKα. Actin was used as a normalization control. (*D*–*G*) In vivo genetic ablation of AMPKα1 and AMPKα2 in the developing cortex. Western blot analysis reveals decreased levels of total AMPKα (1 and 2) in cortical lysates from $Emx1^{Cre/+}$; $AMPK\alpha1^{-/-}$; $AMPK\alpha2^{F/F}$ mice compared with control littermates in cortical tissue (*D*) and dissociated cortical neurons (*E*). Ablation of AMPKα in the cortex results in decreased phosphorylation of $GABA_B$ R2 at residue Ser783 (*F*) as well as the retinoblastoma tumor suppressor gene Rb phosphorylated at Ser807/811 (*G*). Bar graphs represent quantification of indicated protein relative to the nonphosphorylated form of the protein (when appropriate) and/or to α-tubulin or neuron-specific β-tubulin-III (TuJ1). Error bars represent SE to the mean (n = 3).

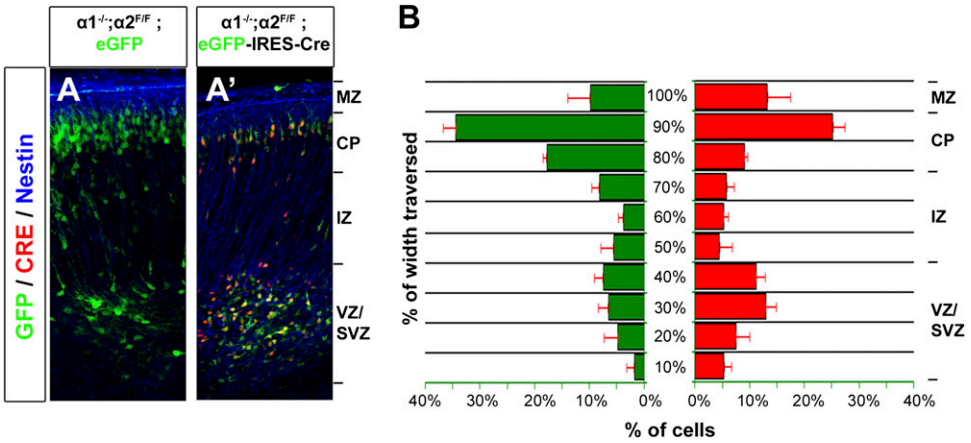

Fig. S2. AMPKα is not required for radial migration of cortical neurons. (*A* and *A′*) E15.5 cortical slices of AMPKα1$^{-/-}$; AMPKα2$^{F/F}$ brains were cultured for 5 d after electroporation with EGFP (control, *A*) or Cre-IRES-EGFP (experimental, *A′*). Slices were stained with anti-nestin antibody revealing radial glial scaffold (blue). MZ, marginal zone; CP, cortical plate; IZ, intermediate zone; VZ, ventricular zone; SVZ, subventricular zone. (*B*) Quantification of three independent experiments of cell distribution for slices expressing EGFP (green bars, *Left*) or Cre-IRES-EGFP (red bars, *Right*).

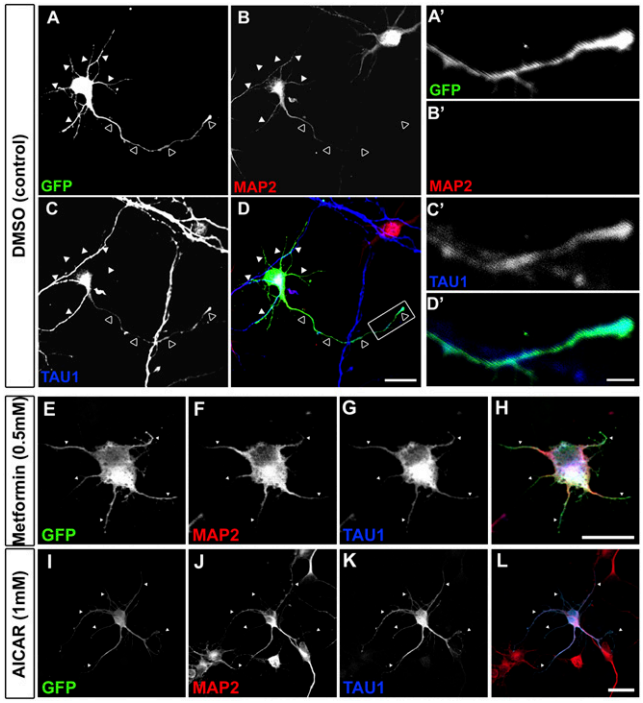

Fig. S3. AMPK activators alter cortical neuron morphology. (*A–D*) Examples of E15.5 cortical neurons electroporated, dissociated, and grown in vitro for 4 d. Neurons were treated for 3 d with vehicle (DMSO) starting at 1 div. Neuron morphology was visualized by GFP expression (*A*). Neurons were stained with the somato-dendritic marker MAP2 (*B*) and the axon marker Tau1 (*C*). White arrow: MAP2 positive, Tau1 negative dendrites. Open arrow: MAP2 negative, Tau1 positive axon. (Scale bar, 25 μm.) (*A′–D′*) Higher magnification of the boxes from *D*. (Scale bar, 3 μm.) (*E–L*) Morphology of neurons treated for 3 d with metformin (0.5 mM) (*E–H*) or AICAR (1 mM) (*I–L*). Neurons were immunostained with GFP (*A*), MAP2 (*B*), and Tau1 (*C*). White arrow: MAP2 and Tau1 positive neurites. (Scale bar, 20 μm.)

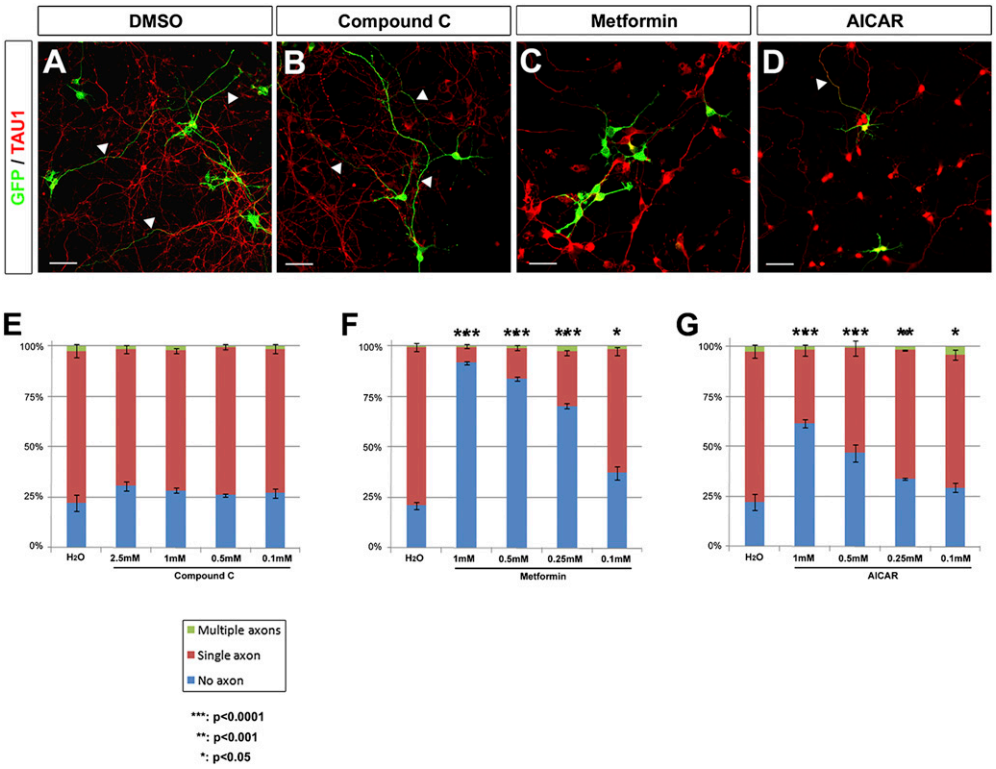

Fig. S4. Metabolic stress impairs axogenesis. (*A–D*) E15.5 cortical neurons electroporated, dissociated, and maintained for 4 div. At 1 div, cells were treated for 3 d with either vehicle (H_2O or DMSO) (*A*), the AMPK inhibitor compound C (5 μM) (*B*), or the AMPK activators metformin (0.5 mM) (*C*) and AICAR (1 mM) (*D*). Neurons grown in control conditions or treated with compound C exhibit a single axon (arrowhead). Note the absence of axons in neurons cultured in the presence of AICAR and metformin, which activates AMPK. (Scale bar, 50 μm.) (*E–G*) Dose-dependent effect of the AMPK inhibitor, compound C (*E*), or activators metformin (*F*) and AICAR (*G*) on neuronal polarity. E15.5 neurons were treated at 1 div for 3 d with the indicated drugs at the indicated concentrations. Quantifications are based on ≥100 neurons per condition. Mean proportion represents neurons with no (blue), one (red), or multiple (green) >100 μm long and Tau1-positive axon for at least three independent experiments. Fisher's exact test was used to statistically analyze the data represented (***$P < 0.001$; *$P < 0.05$).

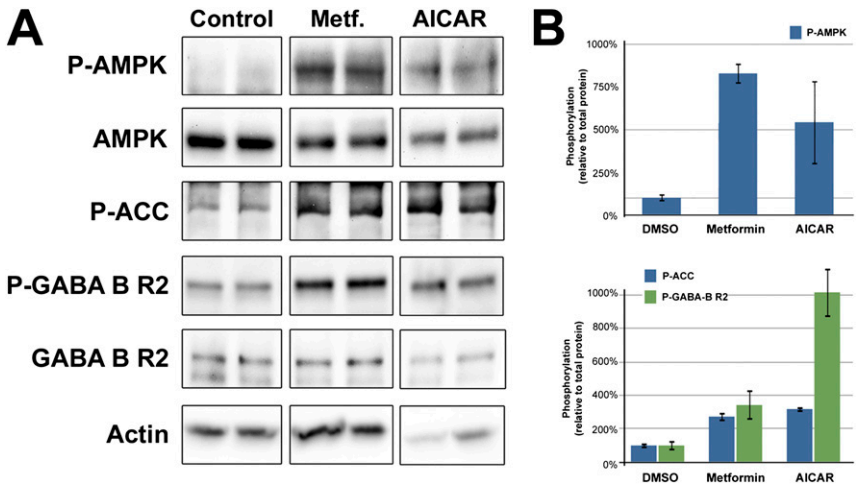

Fig. S5. AMPK activators metformin and AICAR increase AMPK activity in cortical neurons. Western blot analysis after E18.5 dissociated cortical neurons cultured for 1 d in vitro after treatment with metformin (2 mM) or AICAR (2 mM) for 3 consecutive days. Both treatments increased the phosphorylation of AMPKα (Thr172, compare with total AMPKα expression). Treatments also increased the phosphorylation of two downstream targets of AMPK, ACC (Ser79) and $GABA_B$ R2 (Ser783). Actin was used as normalization control.

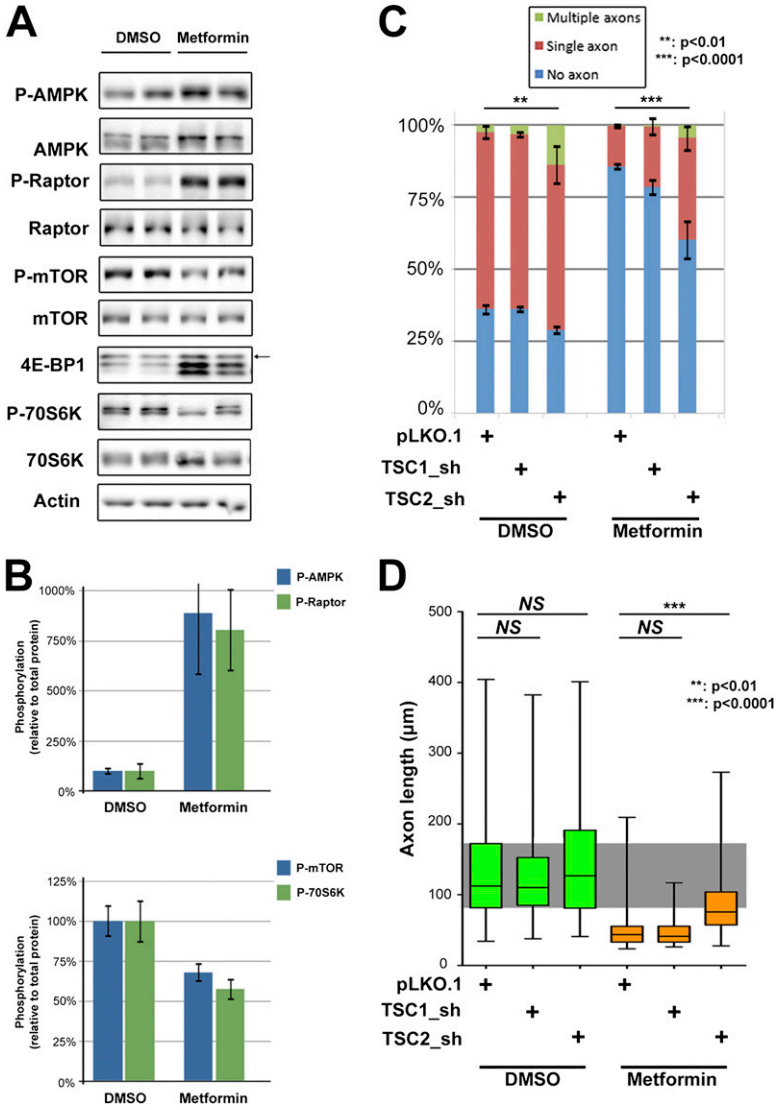

Fig. S6. TSC1 and TSC2 knockdown only partially rescues metformin phenotype. (*A*) Western blot analysis after in vitro culture of E18.5 mouse cortical neurons cultured for 1 d, then treated with metformin (2 mM) for 3 d in vitro. Phosphorylation of AMPK (phospho-Thr172), raptor (phospho-Ser792), mTOR (phospho-Ser2448), p70S6K (phospho-Ser371), and 4E-BP1 were assessed similarly to what is described in Fig. 4. (*B*) Quantification of phospho-AMPK, phospho-raptor, phospho-mTOR, and phospho-70S6K signal were normalized to total amount of corresponding proteins compared with control condition (DMSO vehicle only). Error bars represent SEM ($n = 5$). (*C* and *D*) Quantification of neuronal polarity (*C*) and longest neurite length (*D*) for five independent experiments ($n \geq 500$ for polarization, $n \geq 500$ for length). Statistical analyses were performed using Fisher's exact test (*C*) or one-way ANOVA (*D*).

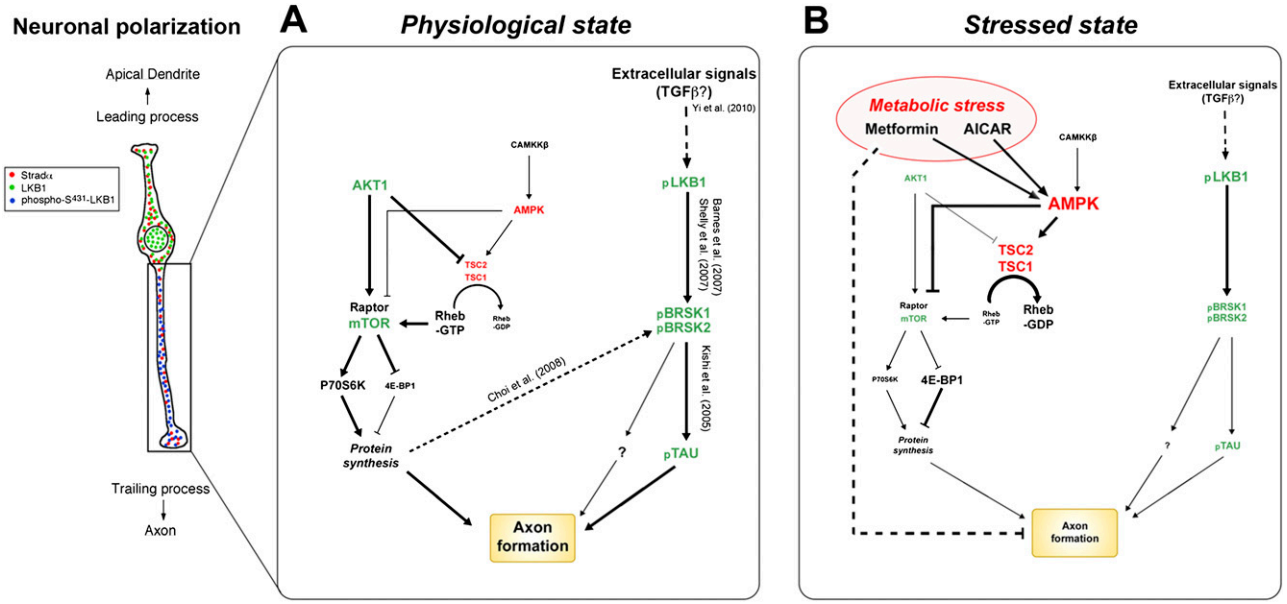

Fig. S7. Model: AMPK overactivation impairs axogenesis during metabolic stress. Synthesis of pathways demonstrated or previously shown to regulate axogenesis both under normal physiological conditions (*A*) or (metabolic) stress-induced states (*B*). Both positive (green) and negative (red) regulators of axon outgrowth intersect to determine net axon outgrowth/specification. During normal mammalian development in vivo (*A*), axon specification and subsequent axon growth requires local phosphorylation of LKB1 on S431 (1, 2) to specify one neurite (future trailing process) to become the axon. This local phosphorylation might be triggered by proteins such as cAMP-dependent kinase (PKA) or other kinases in response to graded extracellular cues such as TGF-β (3). LKB1 phosphorylates and activates AMPK-like proteins such as BRSK1/2 (SAD-A/B) and probably others, which in turn phosphorylate key effectors such as the microtubule-associate protein Tau and probably many other effectors that participate in axon formation (1). Another parallel pathway involving the kinase AKT and AMPK acts as positive and negative regulators of mTOR and local protein synthesis, respectively. AKT has previously been shown to act as a promoter of axogenesis, whereas TSC1/2 have been shown to act as negative regulators of axogenesis in part through mTOR-mediated translation of SAD-A/B (BRSK2/1; ref. 4). Our results show that AMPK is not required constitutively for axon formation or neuronal differentiation but AMPK overactivation under conditions of metabolic stress (mimicked by AICAR or metformin treatments) results in overactivation of TSC2 and inhibition of raptor, which leads to inhibition of axogenesis. See text for further details.

1. Barnes AP, et al. (2007) LKB1 and SAD kinases define a pathway required for the polarization of cortical neurons. *Cell* 129:549–563.
2. Shelly M, Cancedda L, Heilshorn S, Sumbre G, Poo MM (2007) LKB1/STRAD promotes axon initiation during neuronal polarization. *Cell* 129:565–577.
3. Yi JJ, Barnes AP, Hand R, Polleux F, Ehlers MD (2010) TGF-beta signaling specifies axons during brain development. *Cell* 142:144–157.
4. Choi YJ, et al. (2008) Tuberous sclerosis complex proteins control axon formation. *Genes Dev* 22:2485–2495.

Table S1. List of antibodies and concentration used

Target protein	Species	Company	Concentration used
AMPKα	Rabbit	Cell Signaling	1:1,000 (WB)
P-AMPKα (T172)	Rabbit	Cell Signaling	1:1,000 (WB)
Tuj1 (βIII-tubulin)	Mouse	Sigma	1:1,000 (WB, ICC)
$GABA_B$ R2	Rabbit	Cell Signaling	1:1,000 (WB)
$GABA_B$ R2 (S783)	Rabbit	PhosphoSolutions	1:1,000 (WB)
Rb	Mouse	Santa Cruz	1:1,000 (WB)
Rb (S807/811)	Rabbit	Santa Cruz	1:1,000 (WB)
α-Tubulin	Mouse	Sigma	1:15,000 (WB)
CTIP 2	Mouse	Abcam	1:500 (IHC)
Cux1	Rabbit	Santa Cruz	1:500 (IHC)
Tbr1	Rabbit	Chemicon	1:500 (IHC)
Nestin	Mouse	BD-Bioscience	1:2,000 (IHC)
Activated caspase-3	Rabbit	Cell Signaling	1:500 (IHC)
Tau-1	Mouse	Chemicon	1:2,000 (ICC)
MAP2 (a/b isoforms)	Rabbit	Millipore	1:1,000 (IHC); 1:2,000 (ICC)
GFP	Chicken	Upstate	1:1,000 (ICC, IHC)
Cre	Rabbit	Novagen	1:1,000 (IHC)
P-raptor (S792)	Rabbit	Cell Signaling	1:1,000 (WB)
Raptor	Rabbit	Cell Signaling	1:1,000 (WB)
P-mTOR (S2448)	Rabbit	Cell Signaling	1:1,000 (WB)
mTOR	Rabbit	Cell Signaling	1:1,000 (WB)
4E-BP1	Rabbit	Cell Signaling	1:2,000 (WB)
P-70S6K (S371)	Rabbit	Cell Signaling	1:1,000 (WB)
70S6K	Rabbit	Cell Signaling	1:1,000 (WB)
Actin	Mouse	Millipore	1:10,000 (WB)
P-ACC	Rabbit	Cell Signaling	1:1,000 (WB)
ACC	Rabbit	Cell Signaling	1:1,000 (WB)

WB, Western blot; ICC, immunocytochemistry; IHC, immunohistochemistry.